Biosensors and Bioelectronics 25 (2010) 2442–2446

Contents lists available at ScienceDirect

Biosensors and Bioelectronics

journal homepage: www.elsevier.com/locate/bios

Direct electrochemistry and bioelectrocatalysis of horseradish peroxidase based on gold nano-seeds dotted TiO_2 nanocomposite

Yao Wang, Xiaoling Ma, Ying Wen, Yueyi Xing, Zongrang Zhang, Haifeng Yang*

Department of Chemistry, Shanghai Normal University, 100 Guilin Road, Xuhui District, Shanghai 200234, PR China

ARTICLE INFO

Article history:
Received 30 January 2010
Received in revised form 23 March 2010
Accepted 2 April 2010
Available online 10 April 2010

Keywords:
Gold nano-seeds
TiO_2
Horseradish peroxidase
Direct electron transfer
Hydrogen peroxide
Biosensor

ABSTRACT

Gold nano-seeds (GNSs) (Φ = 2–5 nm) were dotted in TiO_2 colloids and the horseradish peroxidase (HRP) was successfully immobilized on the as-made GNSs–TiO_2 nanocomposite by a convenient and effective method. The matrix integrates the merits of both GNSs and TiO_2, which provides a favorable microenvironment for the immobilization of HRP. The cyclic votammetric results demonstrated that the entrapped HRP achieves direct electron transfer at glassy carbon electrode (GCE). A pair of stable and quasi-reversible redox peaks with a small peak-to-peak separation of 43 mV was observed in phosphate buffer solution. The GNSs stabilized by TiO_2 colloids acted sufficiently as the conducting tunnel to promote the electron transfer. As a result, the electrochemical behaviors were improved in virtue of the synergic effect of TiO_2 and GNSs. The Nafion/HRP–GNSs–TiO_2/GCE displayed an excellent and rapid electrocatalytic response to the reduction of H_2O_2. The proposed biosensor exhibited a good linear response in the range from 4.1×10^{-5} to 6.3×10^{-4} mol L^{-1}, with a detection limit of 5.9×10^{-6} mol L^{-1} (at the ration of signal to noise, S/N = 3). The apparent Michaelis–Menten constant was estimated to be 0.63 mmol L^{-1}. Furthermore, the biosensor possesses satisfactory stability and good reproducibility.

1. Introduction

To achieve the direct electron transfer (DET) between the enzyme and the electrode is of great significance in fabrication of mediator-free electrochemical biosensors. However, the catalytic center of an enzyme is deeply embedded in an insulating protein shell which resulting in a sluggish electron-transfer kinetics (Yin et al., 2009). On the other hand, the enzyme generally loss its bioactivity when it is adsorbed directly onto the electrode surface (Hong et al., 2006). These reasons make it difficult to transfer electrons directly at conventional electrodes. Therefore, appropriate promoters should be employed to facilitate the electron transfer and retain the bioactivity of immobilized enzymes.

With the fast development of nanotechnology, various nanomaterials such as metal oxide nanomaterials (Liu et al., 2003; Sun et al., 2009; Qiu et al., 2010) and metal nanoparticles (Yang et al., 2008; Ma et al., 2009; Wang et al., 2009) have been widely used to modify electrodes, which are conducive to realize the direct electron transfer of enzyme. Among these nanoparticles, semiconductor material TiO_2 with its applications in catalyst support and photocatalysis has aroused more and more interest in the past decades. This nanomaterial has diverse existing forms such as nanoparticles (Fu et al., 2005), nanofibers (Jin et al., 2007) and nanotubes (Yao et al., 2003; Zheng et al., 2008). Recently, TiO_2 with various forms were extensively applied in developing biosensors (Zhang et al., 2004; Kafi et al., 2008; Wu et al., 2008; Li et al., 2009). Due to the excellent stability, good biocompatibility, relatively good conductivity and high surface area, TiO_2 nanoparticles are expected to be exploited as a film-forming material. Gold nanoparticles (GNPs) with unique physical and chemical properties have become one of the most popular modifiers employed in the construction of third generation biosensors. Enormous works have reported that GNPs could not only provide a friendly microenvironment to maintain the biocompatibility of immobilized enzymes, but also act as the conducting tunnel to promote the electron transfer (Feng et al., 2005; Li et al., 2008; Zhao et al., 2008a; Xiang et al., 2009; Yin et al., 2009). However, GNPs, especially for the gold nano-seeds (GNSs, Φ < 10 nm) are prone to aggregate in aqueous solution owing to their intrinsic property. Therefore, some control measures should be done to avoid such circumstances.

Horseradish peroxidase (HRP) could be easily available with high purity and sensitivity, which allows the generation of strong signals in a relatively short time span (Veitch, 2004). And it was commonly used to fabricate biosensors for the accurate and reliable determination of H_2O_2 (Lu et al., 2006; Upadhyay et al., 2009). In addition, compared with other measurements, the electrochemical method based on HRP biosensors has been proved to be more convenient and rapider because of their high sensitivity and low

* Corresponding author. Tel.: +86 21 64321701; fax: +86 21 64321701.
E-mail address: haifengyang@yahoo.com (H. Yang).

0956-5663/$ – see front matter © 2010 Elsevier B.V. All rights reserved.
doi:10.1016/j.bios.2010.04.002

detection limit (Yu et al., 2005; Zeng et al., 2009; Zhao et al., 2009). Therefore, excellent bioelectrocatalysis to HRP is vital to the accurate and sensitive detection of H_2O_2. Nafion is a biocompatible proton-conductive polymer which has been exploited as an immobilization matrix for enzyme (Lu et al., 2008; Xiang et al., 2009). It is expected to form a protective film for a robust increase of the mixture, improve the stability and prevent the interference.

In this work, we introduced a convenient and effective method to prepare a GNSs–TiO_2 nanocomposite for the construction of a HRP biosensor on glassy carbon electrode. The GNSs were stabilized by TiO_2 colloids so that the unique framework of TiO_2 could effectively prevent the aggregation of GNSs. Moreover, the GNSs–TiO_2 composite could offer an environment similar to that of the redox proteins in a native system. The resulting nanocomposite combined the characteristics of both TiO_2 and GNSs, which was conducive to retain the bioactivity of HRP and to enhance the electron transfer ability. HRP entrapped in the hybrid film exhibited direct electrochemistry on glassy carbon electrodes. Its electrocatalytic responses to the reduction of H_2O_2 were investigated by cyclic voltammetry and amperometry. The experimental results demonstrated that GNSs and TiO_2 possess synergic effect in the nanocomposite. Moreover, the biosensor showed high sensitivity, good stability and satisfactory reproducibility.

2. Experimental

2.1. Reagents

HRP (EC 1.11.1.7, RZN 3.0, 250 units mg^{-1}) was purchased from Shanghai Lizhu Dongfeng Biotechnology Co., Ltd. (China). TiO_2 P25 (TPN24NMYT) was purchased from Beijing Midwest Group (China). $HAuCl_4$, $NaBH_4$ and trisodium citrate were obtained from Sigma Chemical Co. Phosphate buffer solutions (PBS, 0.1 mol L^{-1}) with various pH values were prepared by mixing the stock solutions of Na_2HPO_4 and KH_2PO_4, then adjusted by NaOH and H_3PO_4 solutions. The supporting electrolyte was 0.1 mol L^{-1} KCl. All solutions were prepared with doubly distilled water.

2.2. Apparatus

Electrochemical measurements were performed with a CHI 750 C electrochemical workstation (Shanghai CH Instruments, China). A conventional three-electrode system was employed with a modified glassy carbon electrode (Φ = 3 mm) as the working electrode, a platinum wire and a saturated calomel electrode (SCE) were used as the auxiliary and reference electrodes, respectively. All experimental solutions were deoxygenated by bubbling highly pure nitrogen and maintained under nitrogen atmosphere during measurements. UV–vis absorbance spectra were recorded on a UV–vis spectrophotometer (UV-760CRT, Shanghai Precision and Scientific Instrument Co., Ltd). Transmission emission microscopy (TEM) image was performed on TEM (JEM-2100, Japan). Field emission scanning electron microscopy (FESEM) (Hitachi S-4800) was used for imaging the topography.

2.3. Preparation of gold nano-seeds (GNSs)

GNSs were prepared as the method described (Brown et al., 1996) with modification by adding 1 mL of 1% trisodium citrate solution to 100 mL icy solution containing 1 mL 1% (w/v) $HAuCl_4$. 1 mL of 0.075% $NaBH_4$ aqueous solution was added under stirring. Subsequently, the ruby-red GNSs solution was obtained. The size of GNSs which ranged from 2 to 5 nm was estimated from TEM result (see Supplementary Fig. S.1). The prepared GNSs were stored in a dark bottle at 4 °C for further use.

2.4. Modification of electrodes

Glassy carbon electrode (GCE) was polished with 0.3 μm alumina slurry and sonicated in doubly distilled water, ethanol and doubly distilled water, respectively. Initially, TiO_2 dispersion (1 μg mL^{-1}) and GNSs (0.1 mg mL^{-1}) were sonicated for 45 s to make the GNSs evenly dispersed onto TiO_2 surface. Then HRP solution (5 mg mL^{-1}) was added to the mixture and the sonication was continued for 15 s so as to obtain a homogeneously HRP–GNSs–TiO_2 solution. The sonication was carried out in an icy bath and the TiO_2, GNSs, and HRP were mixed in the ratio of 4:6:3 (v/v). With a microsyringe, 6 μL of the mixture was dropped onto the GCE and dried in refrigerator with a small bottle covered. Then, the electrode was rinsed carefully with doubly distilled water to remove the physically adsorbed species. Finally, 3 μL Nafion was casted to form a protective film and dried similarly. The obtained electrode was denoted as Nafion/HRP–GNSs–TiO_2/GCE. As the comparison, Nafion/HRP–TiO_2/GCE and Nafion/HRP–GNSs/GCE were fabricated with the similar procedures. The as-prepared electrodes were covered with a small bottle and kept at 4 °C when not in use.

3. Results and discussion

3.1. Morphology characterization

The mixture solution of GNSs–TiO_2 and HRP–GNSs–TiO_2 were characterized by TEM as shown in Fig. 1. The TEM image of GNSs–TiO_2 (Fig. 1a) dispersion clearly showed the presence of numerous GNSs on the surface of TiO_2, suggesting GNSs could be easily adsorbed onto TiO_2. Due to the larger surface area and stable film-forming property (see Supplementary Fig. S.2), the GNSs–TiO_2 composite was beneficial for the incorporation of HRP (Fig. 1b). Furthermore, GNSs in both GNSs–TiO_2 and HRP–GNSs–TiO_2 composite were well dispersed on the surface of TiO_2 without aggregation. The anti-aggregation effect of HRP–GNSs–TiO_2 composite on GCE was also observed from FESEM characterization (Fig. 1c). These results demonstrated that the TiO_2 in the composite could effectively prevent the aggregation of GNSs.

3.2. UV–vis spectroscopic characterization

Fig. 2 shows the UV–vis spectra of different solutions. The absorption peak of GNSs was located at 517 nm (Fig. 2b), which is a characteristic peak of the surface plasma oscillation of spherical GNPs (Alvarez et al., 1997). While the spectroscopic response of TiO_2 solution did not show an absorption peak (Fig. 2a). When TiO_2 was mixed with GNSs (Fig. 2d), no major change in absorption peak was observed, which suggested that GNSs are uniformly dispersed in the TiO_2 solution and GNSs did not change its characteristic when mixing.

UV–vis spectroscopy is widely used to monitor the possible change of the Soret absorption band of heme group, since it is sensitive to the variation of the microenvironment around the heme site. (George and Hanania, 1953; Zhang et al., 2007; Zhao et al., 2008b). The UV–vis spectrum of native HRP gave a typical heme band at 401 nm (Fig. 2c). For the mixture of HRP–GNSs–TiO_2, the absorption band was observed at 403 nm. Only 2 nm's shift suggested that the structure of HRP in the GNSs–TiO_2 composite was similar to the native state of HRP alone. In addition, we noticed that the Q and CT band definitely occur at about 500 and 640 nm as the week bands respectively in the UV–vis spectrum recorded from Free HRP molecules. Such two broad bands could be observable in UV–vis experimental results of HRP–TiO_2, HRP–GNSs and HRP–GNSs–TiO_2, evidencing that HRP kept its natural structure and bioactivity in

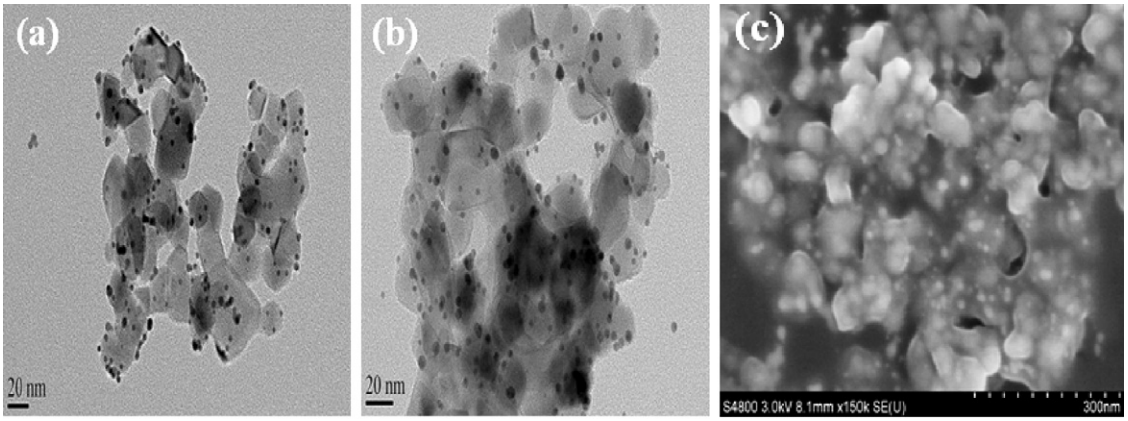

Fig. 1. TEM images of (a) GNSs–TiO_2 and (b) HRP–GNSs–TiO_2, FESEM image of (c) HRP–GNSs–TiO_2 on GCE.

the mixture. Furthermore, we can know that GNSs–TiO_2 had some specific interaction with HRP.

It should be mentioned that a high scattering band of TiO_2 particles at lower wavelengths was observed, but it slightly effected on the band position of HRP (see Supplementary Fig. S.3).

3.3. Direct electrochemistry of Nafion/HRP–GNSs–TiO_2/GCE

Fig. 3 shows the cyclic voltammograms (CVs) of different electrodes in 0.1 mol L^{-1} pH 7.0 PBS at the scan rate of 100 mV s^{-1}. There is no peak observed at the Nafion/GNSs–TiO_2/GCE (Fig. 3a), while the Nafion/HRP–GNSs–TiO_2/GCE (Fig. 3d) displayed a pair of well-defined and quasi-reversible redox peaks. Less stable redox peaks were observed at the Nafion/HRP–GNSs/GCE (Fig. 3c) and Nafion/HRP–TiO_2/GCE (Fig. 3b). Comparing the current response obtained at these modified electrodes, the results suggest that both TiO_2 and GNSs can enhance the electrochemical response of HRP to some extent. Better voltammetric response of HRP at GNSs–TiO_2 film showed advantage over that of TiO_2 and GNSs alone, which could be attributed to the synergic effect of GNSs and TiO_2. The GNSs–TiO_2 composite played an important role as an electron promoter so that the direct electron transfer was successfully established between the electrode and the HRP.

The anodic peak potential (E_{pa}) and the cathodic peak potential (E_{pc}) are located at −0.359 and −0.402 V, respectively. The formal potential ($E^{0'}$, the average of E_{pa} and E_{pc}) is −0.380.5 V. The results of CVs indicated the pair of peaks is a characteristic of Fe (III)/Fe (II) redox couple of the heme protein. The small peak-to-peak separation of 43 mV indicated a fast electron transfer rate, revealing that the GNSs–TiO_2 composite can provide a favorable microenvironment for HRP to undergo a facile electron-transfer reaction.

CVs of Nafion/HRP–GNSs–TiO_2/GCE in pH 7.0 PBS at different scan rates were investigated (see Supplementary Fig. S.4). Both the anodic (i_{pa}) and cathodic (i_{pc}) peak currents are linearly proportional to the scan rates in the range from 100 to 1000 mV s^{-1}, as shown in the inset of Fig. S.2 (linear regression equations: i_{pa} (μA) = 0.03988 + 0.00162 ν (mV s^{-1}), R^2 = 0.998; i_{pc} (μA) = −0.00788–0.0023 ν (mV s^{-1}), R^2 = 0.999), indicating that the electrode reaction corresponds to a surface-confined quasi-reversible process (Chen et al., 2009). In addition, the FESEM characterization of HRP–GNSs–TiO_2 on glassy carbon electrode also suggested that the mixture solution formed a three-dimensional film on the electrode surface, which was beneficial to mass and the direct electron transfers in the interface.

The influence of the solution pH on the electrochemistry behavior of Nafion/HRP–GNSs–TiO_2/GCE was further studied (see Supplementary Fig. S.5). Stable and well-defined CVs could be observed in the pH range from 4.0 to 9.0. With the increase of pH value, both the anodic and cathodic peaks shifted to the negative. The slope from the linear plot of $E^{0'}$ versus pH (inset of Fig. S.3) was about −47.9 mV pH^{-1}. This value was smaller than the theoretical value of −58.0 mV pH^{-1} for a single proton transfer coupled to a quasi-reversible single electron transfer. The possible reason could be ascribed to the influence of the protonation of the water molecule coordinated to the central iron, or the protonation state of trans ligands around the heme group (Yamazaki et al., 1978).

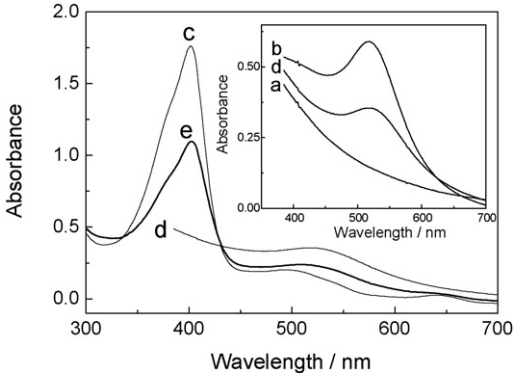

Fig. 2. UV–vis spectra of different solutions: (a) TiO_2, (b) GNSs, (c) HRP, (d) GNSs–TiO_2 (3:2 in v/v) and (e) HRP–GNSs–TiO_2 (3:6:4 in v/v). Sizes for TiO_2 particles (0.051 μg mL^{-1}) ranging from 20 to 60 nm and for GNSs (0.077 mg mL^{-1}) from 2 to 5 nm.

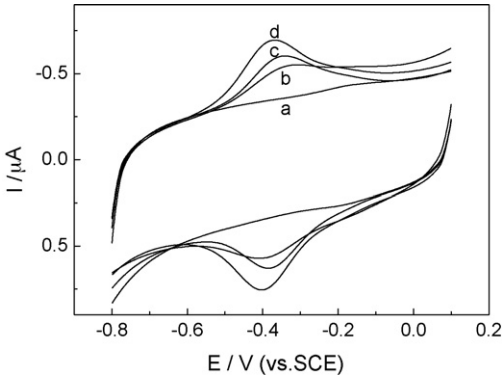

Fig. 3. Cyclic voltammograms of (a) Nafion/GNSs–TiO_2, (b) Nafion/HRP–TiO_2, (c) Nafion/HRP–GNSs and (d) Nafion/HRP–GNSs–TiO_2 modified GCEs in PBS (pH 7.0). Scan rate: 100 mV s^{-1}.

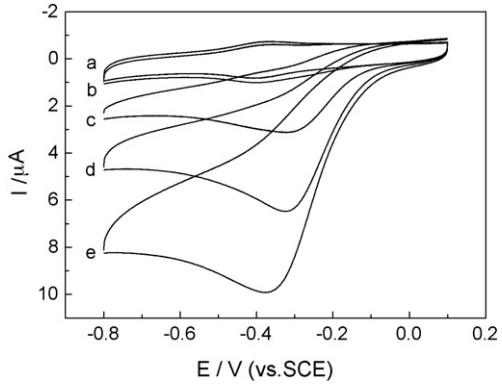

Fig. 4. Cyclic voltammograms of the Nafion/HRP–GNSs–TiO_2/GCE in PBS (pH 7.0) in the absence (a) and presence of (b) 1×10^{-5} mol L^{-1}, (b) 1.0×10^{-4} mol L^{-1}, (c) 3.0×10^{-4} mol L^{-1} and (d) 5.0×10^{-4} mol L^{-1} H_2O_2. Scan rate: 100 mV s^{-1}.

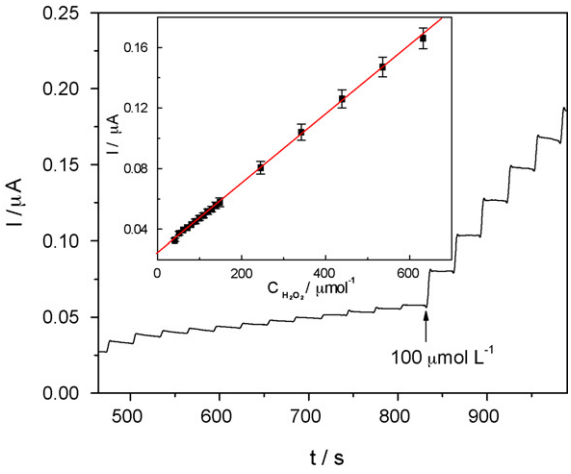

Fig. 5. Amperometric responses of the Nafion/HRP–GNSs–TiO_2/GCE at −0.3 V upon successive additions of H_2O_2 to PBS (pH 7.0) with stirring. Inset: calibration curve between current and H_2O_2 concentration.

3.4. Electrochemical response of the Nafion/HRP–GNSs–TiO_2/GCE to H_2O_2

The catalytic reduction of H_2O_2 at the Nafion/HRP–GNSs–TiO_2/GCE was also studied. As shown in Fig. 4, the reduction peak increases dramatically with the addition of H_2O_2, accompanied by a decrease and disappearance of the oxidation peak. These results indicated that the immobilized HRP presents a good electrocatalytic activity toward H_2O_2. The electrocatalytic reduction of H_2O_2 at Nafion/HRP–GNSs–TiO_2/GCE, Nafion/HRP–GNSs/GCE and Nafion/HRP–TiO_2/GCE were compared (see Supplementary Fig. S.6). As expected, in the presence of same H_2O_2 concentration, the proposed biosensor Nafion/HRP–GNSs–TiO_2/GCE possessing composite nanoparticles presented better catalytic ability and wider detection range than those electrodes possessing only one kind of nanoparticles alone. The higher sensitivity and wider detection range are attributed to the larger amount of HRP loading on the GNSs–TiO_2 composite, which is in agreement with the previous report (Li et al., 2009).

The amperometric responses of the Nafion/HRP–GNSs–TiO_2/GCE with successive additions of H_2O_2 to PBS (pH 7.0) at an applied potential of −0.3 V is shown in Fig. 5. The current response of the biosensor increased along with H_2O_2 concentration. The Nafion/HRP–GNSs–TiO_2/GCE reached 95% of the steady-state current within 3 s, indicating a rapid electrocatalytic response. The calibration curve obtained for H_2O_2 (inset of Fig. 5) showed a linear range from 4.1×10^{-5} to 6.3×10^{-4} mol L^{-1} with a correlation coefficient of 0.999 ($n = 17$). A detection limit of 5.9×10^{-6} mol L^{-1} was obtained at the ratio of signal to noise of 3.

The apparent Michaelis–Menten constant (K_M^{app}), an indication of the enzyme–substrate kinetics, is generally used to evaluate the biological activity of an immobilized enzyme (Zou et al., 2008). The K_M^{app} can be obtained by the Lineweaver–Burk equation (Kamin and Wilson, 1980):

$$\frac{1}{I_{ss}} = \frac{K_M^{app}}{I_{max}C} + \frac{1}{I_{max}} \quad (1)$$

where I_{ss} is the steady-state current after the addition of substrate, C is the bulk concentration of the substrate, and I_{max} is the maximum current measured under saturated substrate conditions. K_M^{app} can be obtained by the analysis of slope and intercept of the plot of the reciprocals of the steady-state current versus H_2O_2 concentration. The K_M^{app} value for Nafion/HRP–GNSs–TiO_2/GCE was estimated to be 0.63 mmol L^{-1}, smaller than that of 1.22 mmol L^{-1} for HRP–AuNPs–SF/GCE (Yin et al., 2009), 1.76 mmol L^{-1} for ZnO–GNPs–Nafion–HRP/GCE (Xiang et al., 2009), 23.15 mmol L^{-1} for Clay–HRP–Clay/AuCS–GCE (Zhao et al., 2008b). These results suggest that the Nafion/HRP–GNSs–TiO_2/GCE possesses a higher biological affinity to H_2O_2. However, this K_M^{app} value was higher than that of 0.2 mmol L^{-1} for HRP–TiO_2/PGE (Zhang et al., 2004), which maybe ascribed to the partial adsorption of HRP on bulk GCE surface and decreased its affinity for H_2O_2. Table 1 lists different H_2O_2 biosensors employed TiO_2 nanoparticles as a mobilization substrate. We could find that the linear detection rage, response time and K_M^{app} of the Nafion/HRP–GNSs–TiO_2/GCE are in a relatively good position compared to other TiO_2 or gold nanoparticle modified electrodes. The comparison indicated that the proposed convenient method which could effectively prevent the gold nanoparticles from aggregation was a promising way to develop H_2O_2 biosensors.

3.5. Stability and reproducibility

The stability of the Nafion/HRP–GNSs–TiO_2/GCE was investigated. No obvious change of CV curve could be observed even 100

Table 1
Comparison of the performances of different H_2O_2 biosensors employed TiO_2 nanoparticles as a mobilization substrate.

Modified electrode	Linear range (μmol L^{-1})	Detection limit (μmol L^{-1})	Response time (s)	K_M^{app} (mmol L^{-1})	Reference
Nafion/HRP–GNSs–TiO_2/GCE	41–630	5.9	3	0.63	This work
Hb/CMC–TiO_2–NTs/GCE	4–64	4.6	10	Not reported	Zheng et al. (2008)
HRP/Au/TiO_2/Ti	5–400	2.0	5	Not reported	Kafi et al. (2008)
HRP–TiO_2/PGE	7.5–123	2.5	Not reported	0.2	Zhang et al. (2004)
HRP/TiO_2/NTAs	0.5–10 and 50–1000	0.1	Not reported	1.9	Wu et al. (2008)
HRP/3DOM GTD/ITO	0.5–1400	0.2	3	Not reported	Li et al. (2009)
TiO_2 sol–gel/HRP/GCE	80–560	1.5	5	1.89 ± 0.21	Yu and Ju (2002)

Hb, hemoglobin; CMC, carboxymethyl cellulose; TiO_2–NTs, TiO_2 nanotubes; PGE, pyrolytic graphite electrode; NTAs, nanotube arrays; 3DOM, three-dimensionally ordered macroporous; GTD, gold-nanoparticle-doped titanium dioxide; ITO, indium–tin oxide.

continuous cyclic scans were repeated in the potential range from −0.8 to 0.1 V with a scan rate of 300 mV s^{-1} (see Supplementary Fig. S.7). The biosensor could retain 90.1% of its initial response after 2 weeks storage (see Supplementary Fig. S.8).

The reproducibility of the biosensor was investigated by determining 0.1 mmol L^{-1} H_2O_2 in PBS (pH 7.0). The relative standard deviation (R.S.D.) was 4.0% for 7 successive assays. The fabrication reproducibility for three electrodes gave an R.S.D. of 4.2% for the determination of 0.1 mmol L^{-1} H_2O_2. These results suggested that the proposal biosensor possessed good stability and repeatability, which could be satisfactorily used in the determination of H_2O_2.

4. Conclusions

HRP, as a model enzyme, was successfully immobilized on a new biocompatible nanocomposite composed of TiO_2 and GNSs. Morphology characterization demonstrated that TiO_2 in the hybrid film could effectively prevent the aggregation of GNSs. The nanocomposite could not only offer a favorable environment to immobilize HRP but also facilitate the electron transfer between HRP and underlying GCE. Direct electrochemistry of HRP and its bioelectrocatalysis to the reduction of H_2O_2 was realized in virtue of the improved stability and conductivity of mixed nanoparticles. The nanocomposite exhibited advantages over TiO_2 and GNSs alone in fabricating biosensors. Moreover, the biosensor based on the HRP–GNSs–TiO_2 biocomposite film showed such characteristics as fast response, high sensitivity and good stability. This work is expected to provide a new strategy for developing other enzyme-based biosensor.

Acknowledgements

This work was supported by the National Natural Science Foundation of China (Grant No. 20975068), Key Laboratory of Resource Chemistry of Ministry of Education, and the Foundation of Shanghai Normal University (Grant No. DYL200703).

Appendix A. Supplementary data

Supplementary data associated with this article can be found, in the online version, at doi:10.1016/j.bios.2010.04.002.

References

Alvarez, M.M., Khoury, J.T., Schaaff, T.G., Shafigullin, M.N., Vezmar, I., Whetten, R.L., 1997. J. Phys. Chem. B 101, 3706–3712.
Brown, K.R., Fox, A.P., Natan, M.J., 1996. J. Am. Chem. Soc. 118, 1154–1157.
Chen, X.H., Hu, J.Q., Chen, Z.W., Feng, X.M., Li, A.Q., 2009. Biosens. Bioelectron. 24, 3448–3454.
Feng, J.J., Zhao, G., Xu, J.J., Chen, H.Y., 2005. Anal. Biochem. 342, 280–286.
Fu, G.F., Vary, P.S., Lin, C.T., 2005. J. Phys. Chem. B 109, 8889–8898.
George, P., Hanania, G., 1953. Biochem. J. 55, 236–243.
Hong, J., Ghourchian, H., Moosavi-Movahedi, A.A., 2006. Electrochem. Commun. 8, 1572–1576.
Jin, M., Zhang, X.T., Nishimoto, S., Liu, Z.Y., Tryk, D.A., Emeline, A.V., Murakami, T., Fujishima, A., 2007. J. Phys. Chem. C 111, 658–665.
Kafi, A.K.M., Wu, G.S., Chen, A.C., 2008. Biosens. Bioelectron. 24, 566–571.
Kamin, R.A., Wilson, G.S., 1980. Anal. Chem. 52, 1198–1205.
Li, J.L., Han, T., Wei, N.N., Du, J.Y., Zhao, X.W., 2009. Biosens. Bioelectron. 25, 773–777.
Li, J.X., Zhou, L.H., Han, X., Liu, H.L., 2008. Sens. Actuator B 135, 322–326.
Liu, B.H., Cao, Y., Chen, D.D., Kong, J.L., Deng, J.Q., 2003. Anal. Chim. Acta 478, 59–66.
Lu, X.B., Zhang, H.J., Ni, Y.W., Zhang, Q., Chen, J.P., 2008. Biosens. Bioelectron. 24, 93–98.
Lu, X.B., Zhang, Q., Zhang, L., Li, J.H., 2006. Electrochem. Commun. 8, 874–878.
Ma, L.P., Yuan, R., Chai, Y.Q., Chen, S.H., 2009. J. Mol. Catal. B: Enzyme 56, 215–220.
Qiu, J.D., Peng, H.P., Liang, R.P., Xia, X.H., 2010. Biosens. Bioelectron. 25, 1447–1453.
Sun, W., Zhai, Z.Q., Wang, D.D., Liu, S.F., Jiao, K., 2009. Bioelectrochemistry 74, 295–300.
Upadhyay, A.K., Ting, T.W., Chen, S.M., 2009. Talanta 79, 38–45.
Veitch, N.C., 2004. Phytochemistry 65, 249–259.
Wang, J.W., Wang, L.P., Di, J.W., Tu, Y.F., 2009. Talanta 77, 1454–1459.
Xiang, C.L., Zou, Y.J., Sun, L.X., Xu, F., 2009. Sens. Actuator B 136, 158–162.
Wu, F.H., Xu, J.J., Tian, Y., Hu, Z.C., Wang, L.W., Xian, Y.Z., Jin, L.T., 2008. Biosens. Bioelectron. 24, 198–203.
Yamazaki, I., Araiso, T., Hayashi, Y., Yamada, H., Makino, R., 1978. Adv. Biophys. 11, 249–281.
Yang, G., Yuan, R., Chai, Y.Q., 2008. Colloid. Surf. B 61, 93–100.
Yao, B.D., Chan, Y.F., Zhang, X.Y., Zhang, W.F., Yang, Z.Y., Wang, N., 2003. Appl. Phys. Lett. 82, 281–283.
Yin, H.S., Ai, S.Y., Shi, W.J., Zhu, L.S., 2009. Sens. Actuator B 137, 747–753.
Yu, J.H., Ju, H.X., 2002. Anal. Chem. 74, 3579–3583.
Yu, P., Lin, Y.Q., Xiang, L., Su, L., Zhang, J., Mao, L.Q., 2005. Langmuir 21, 9000–9006.
Zeng, X.D., Li, X.F., Liu, X.Y., Liu, Y., Luo, S.L., Kong, B., Yang, S.L., Wei, W.Z., 2009. Biosens. Bioelectron. 25, 896–900.
Zhang, H., Xu, J.J., Chen, H.Y., 2007. J. Phys. Chem. C 111, 16564–16570.
Zhang, Y., He, P.L., Hu, N.F., 2004. Electrochim. Acta 49, 1981–1988.
Zhao, H.Y., Zheng, W., Meng, Z.X., Zhou, H.M., Xu, X.X., Li, Z., Zheng, Y.F., 2009. Biosens. Bioelectron. 24, 2352–2357.
Zhao, X.J., Mai, Z.B., Kang, X.H., Dai, Z., Zou, X.Y., 2008a. Electrochim. Acta 53, 4732–4739.
Zhao, X.J., Mai, Z.B., Kang, X.H., Zou, X.Y., 2008b. Biosens. Bioelectron. 23, 1032–1038.
Zheng, W., Zheng, Y.F., Jin, K.W., Wang, N., 2008. Talanta 74, 1414–1419.
Zou, Y.J., Xiang, C.L., Sun, L.X., Xu, F., 2008. Biosens. Bioelectron. 23, 1010–1016.